Influence of Ferroelectric Quantum Criticality on the Charge Distribution at $SrTiO_3$ Interfaces

Amany Raslan
Patrick Lafleur
Bill Atkinson

Raslan *et al*, Phys. Rev. B 95, 054106 (2017)
Atkinson *et al*, Phys. Rev. B 95, 054107 (2017)

STO/LTO interfaces are self-doping

surface charge from:

- polar catastrophe
- O-vacancies
- gating

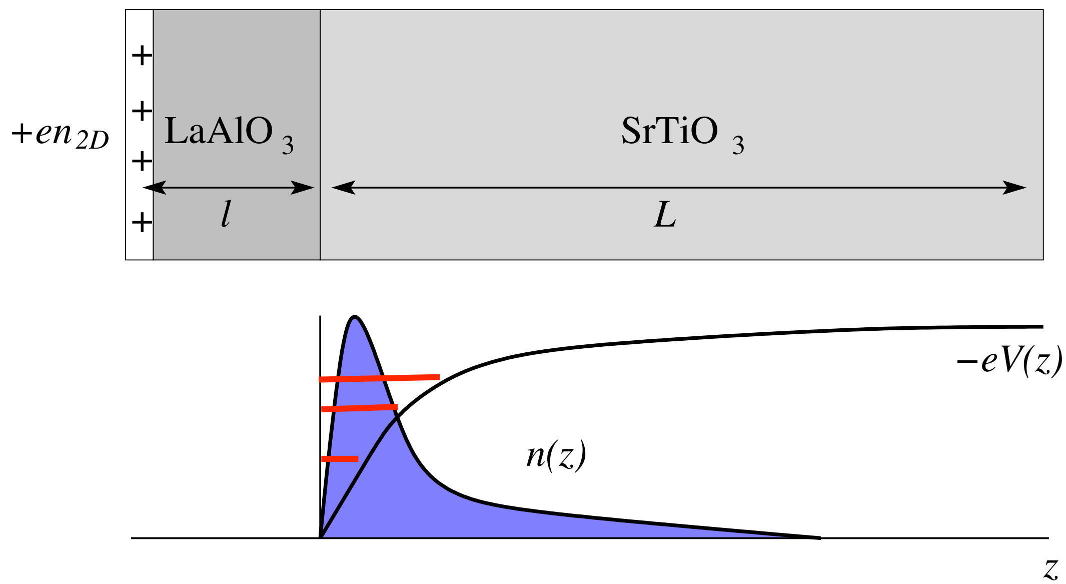

creates confining potential

- quantum interface states
- semiclassical tails (?)

Doping Dependence

Gate control of

- superconductivity
- magnetism
- spin-orbit effects

Caviglia, Nature **456**, 07576 (2008)

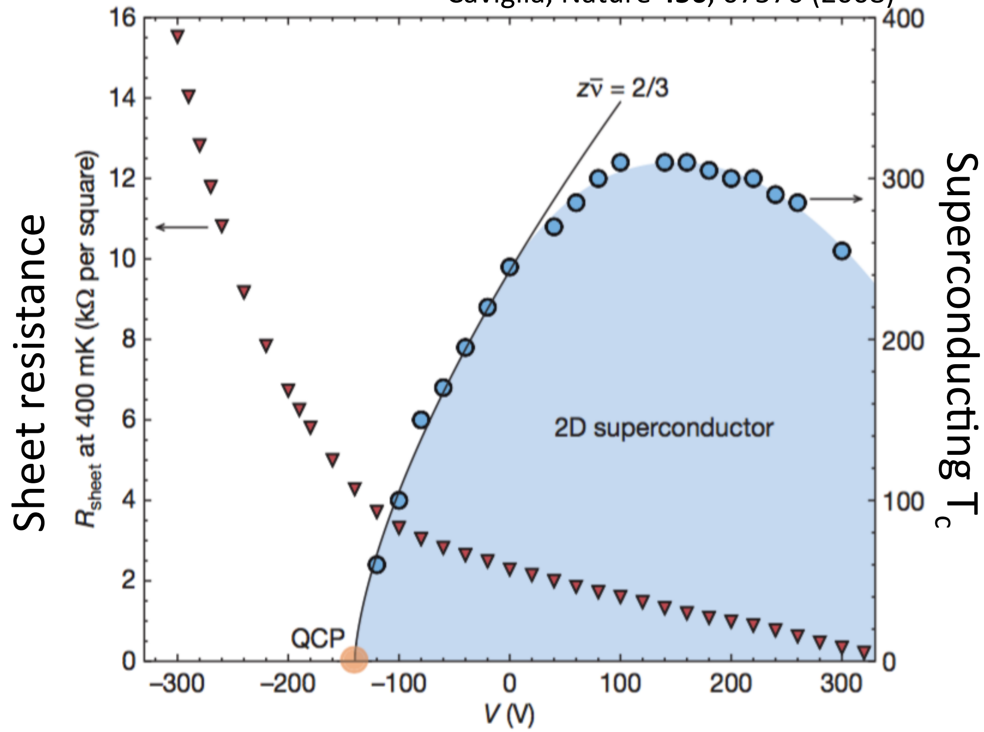

Figure 3 | Electronic phase diagram of the $LaAlO_3/SrTiO_3$ interface. Critical temperature T_{BKT} (right axis, blue dots) is plotted against gate voltage, revealing the superconducting region of the phase diagram. The solid line describes the approach to the quantum critical point (QCP) using the scaling relation $T_{BKT} \propto (V - V_c)^{z\bar{\nu}}$, with $z\bar{\nu} = 2/3$. Also plotted is normal-state sheet resistance, measured at 400 mK (left axis, red triangles) as a function of gate voltage.

Quantum Paraelectricity

VOLUME 26, NUMBER 14 PHYSICAL REVIEW LETTERS 5 APRIL 1971

Dielectric Properties of $SrTiO_3$ at Low Temperatures

T. Sakudo and H. Unoki
Electrotechnical Laboratory, Tanashi, Tokyo, Japan
(Received 8 February 1971)

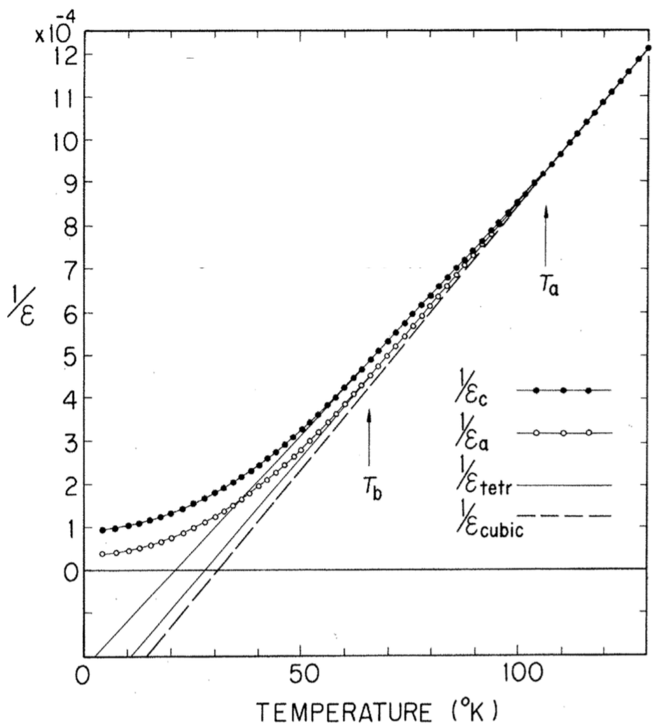

FIG. 3. Inverse dielectric constants as function of temperature. Between T_a and T_b, both ϵ_a^{-1} and ϵ_c^{-1} follow straight lines which are denoted as ϵ_{tetr}^{-1}. Inset: $(\epsilon_i^{-1} - \epsilon_{tetr}^{-1})^{1/2}$ versus temperature, open and solid circles corresponding to ϵ_a and ϵ_c, respectively.

Curie-Weiss $1/\varepsilon \sim T - T_0$

Quantum Paraelectricity

VOLUME 26, NUMBER 14 PHYSICAL REVIEW LETTERS 5 APRIL 1971

Dielectric Properties of $SrTiO_3$ at Low Temperatures

T. Sakudo and H. Unoki
Electrotechnical Laboratory, Tanashi, Tokyo, Japan
(Received 8 February 1971)

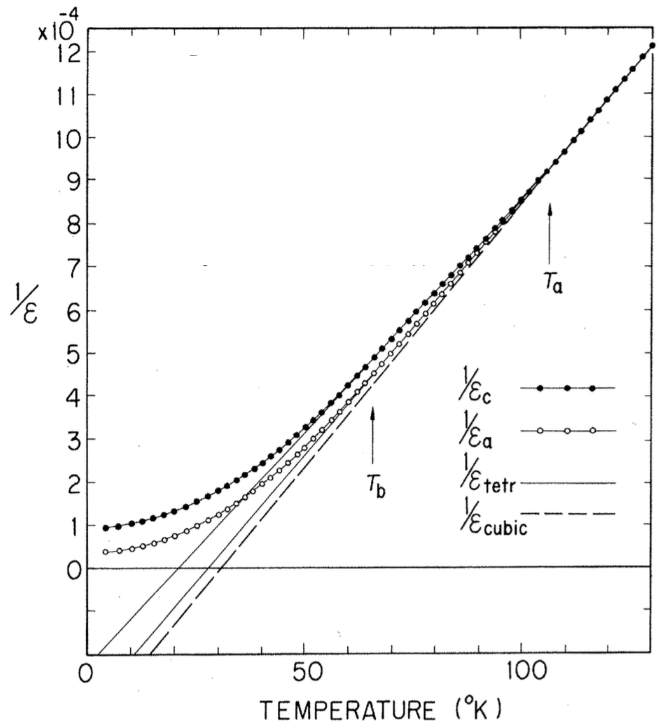

FIG. 3. Inverse dielectric constants as function of temperature. Between T_a and T_b, both ϵ_a^{-1} and ϵ_c^{-1} follow straight lines which are denoted as ϵ_{tetr}^{-1}. Inset: $(\epsilon_i^{-1}-\epsilon_{tetr}^{-1})^{1/2}$ versus temperature, open and solid circles corresponding to ϵ_a and ϵ_c, respectively.

Curie-Weiss $1/\varepsilon \sim T - T_0$

Tetragonal Distortion (2.1°)

(b)

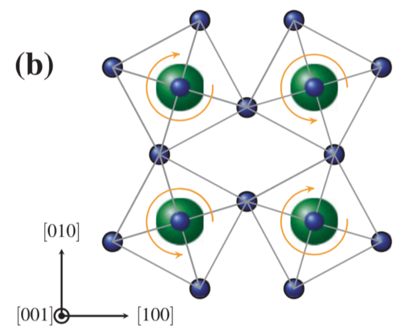

Quantum Paraelectricity

VOLUME 26, NUMBER 14 PHYSICAL REVIEW LETTERS 5 APRIL 1971

Dielectric Properties of $SrTiO_3$ at Low Temperatures

T. Sakudo and H. Unoki
Electrotechnical Laboratory, Tanashi, Tokyo, Japan
(Received 8 February 1971)

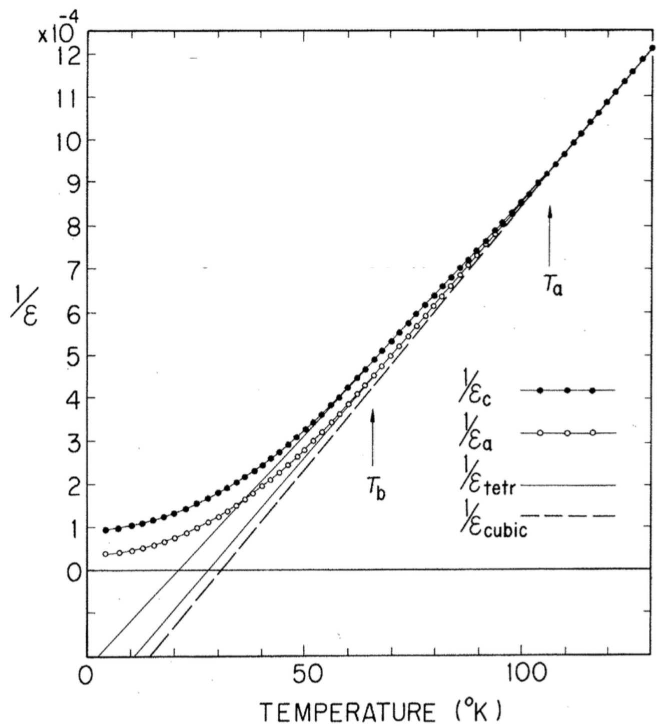

FIG. 3. Inverse dielectric constants as function of temperature. Between T_a and T_b, both ϵ_a^{-1} and ϵ_c^{-1} follow straight lines which are denoted as ϵ_{tetr}^{-1}. Inset: $(\epsilon_i^{-1}-\epsilon_{tetr}^{-1})^{1/2}$ versus temperature, open and solid circles corresponding to ϵ_a and ϵ_c, respectively.

Curie-Weiss $1/\varepsilon \sim T - T_0$

Tetragonal Distortion (2.1°)

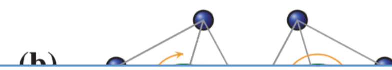

Onset of quantum fluctuations

$$1/\varepsilon = a + bT^2$$

$SrTiO_3$ is close to a quantum critical point

Why do we care about quantum criticality?

- Near the QCP, the properties of the 2DEG should reflect the properties of the QCP.

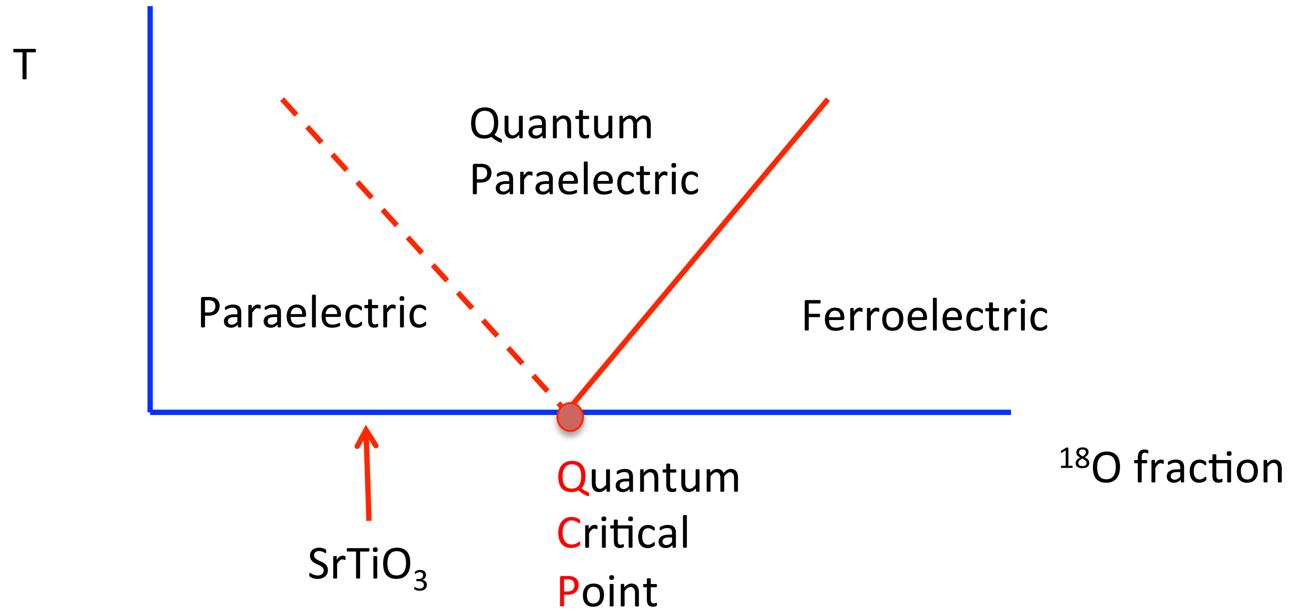

$$\left(-\frac{\partial^2}{\partial z^2}+\xi^{-2}\right)P(z)=\varepsilon_\infty \xi_0^{-2}E(z) \qquad \xi^{-2}(T,P)=\xi^{-2}(0)+AT^{2\nu}+BP^{\delta-1}$$

$$\xi_0 \sim 1 \ \mathring{A}$$

Our calculations

Gauss' Law:

$$-\varepsilon_\infty \frac{\partial^2 V}{\partial z^2} = -en(z) - \frac{\partial P}{\partial z}$$

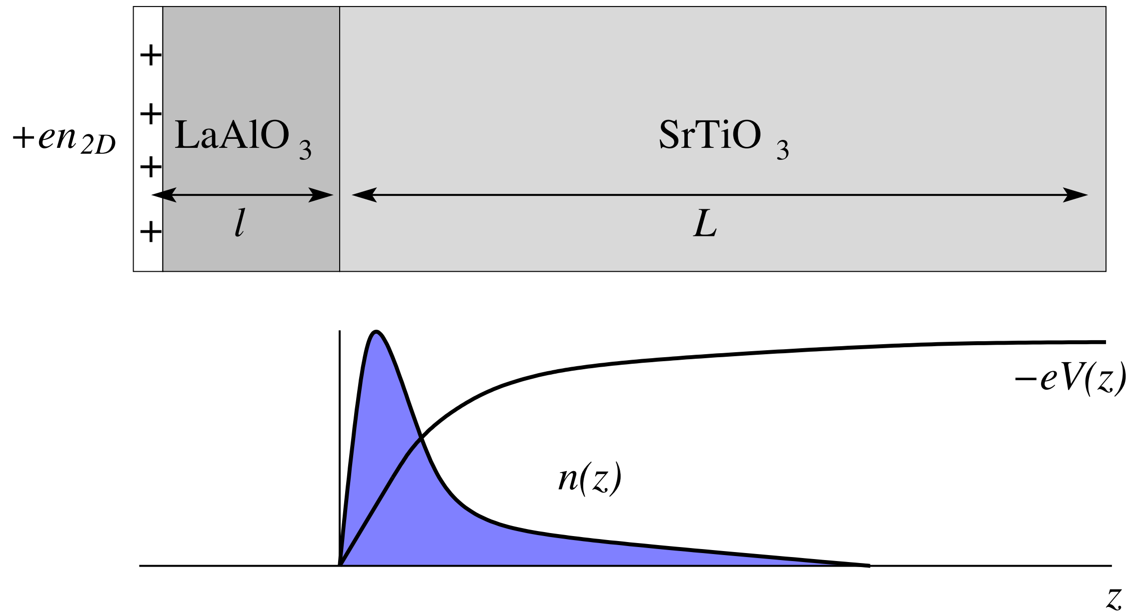

Schrodinger Equation:

$$H_0 = -\sum_{\langle i,j\rangle,\alpha} t_{ij}^{\alpha} c_{i\alpha}^{+} c_{j\alpha} - e\sum_{i\alpha} V_i n_{i\alpha}$$

Phonon model:

$$H_{\text{lattice}} = \sum_{i\alpha}\frac{\Pi_{i\alpha}^2}{2M} + \frac{1}{2}\sum_{ij\alpha} X_{i\alpha} D_{ij}^{0\alpha} X_{j\alpha} + \frac{B}{4\eta}\sum_{i}\left(\sum_{\alpha} X_{i\alpha}^2\right)^2 - Q\sum_{i\alpha} E_{i\alpha} X_{i\alpha}$$

after Schneider et al, PRB 13, 1123 (1976)

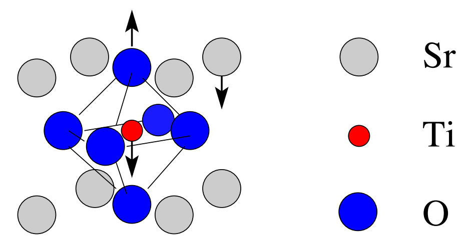

$$P_{i\alpha} = \frac{Q\langle X_{i\alpha}\rangle}{a_0^3}$$

Self-consistent solutions for the charge density

High Density

Typical density

Low density
(near MIT)

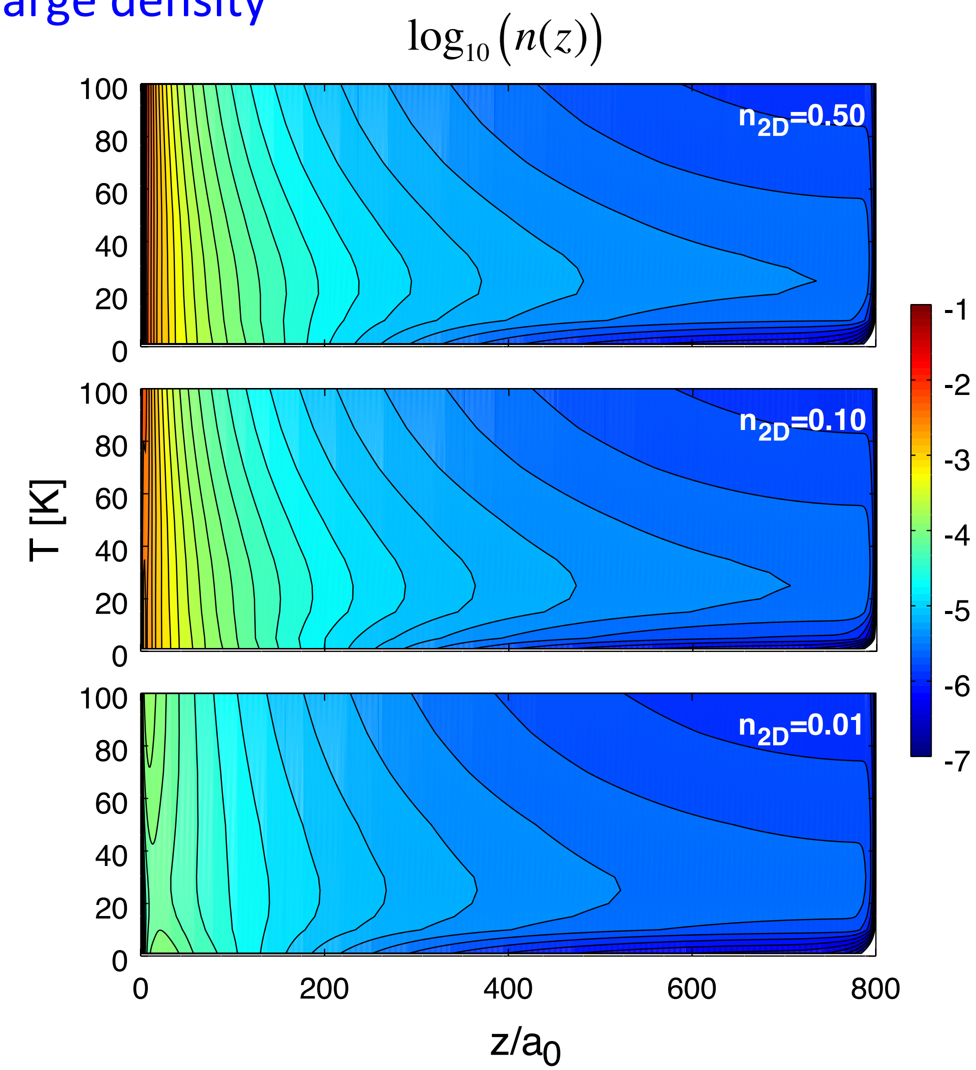

TRENT UNIVERSITY

Self-consistent solutions for the charge density

- Universal tails extend 100's of unit cells into bulk.
- Nonmonotonic T-dependence
- No interfacial component at low n_{2D}

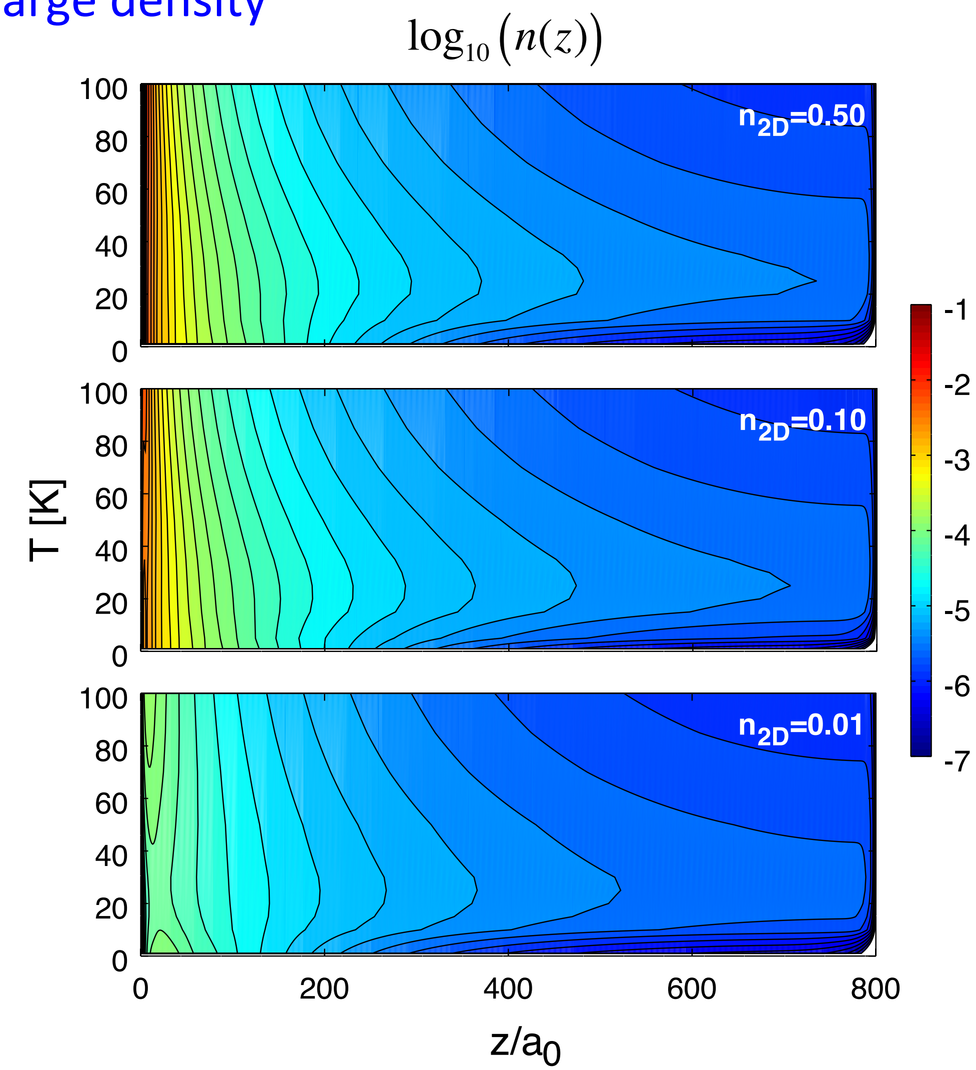

Why?

Solution in the weak-field limit:

$$n(z) \approx n_{2D} \frac{\lambda(T)}{[\lambda(T)+z]^2}$$

where the length scale is

$$\lambda(T) = \frac{\varepsilon_\infty 2k_B T \xi(T)^2}{n_{2D} e^2 \xi_0^2}$$

$$\sim \frac{T}{\xi^{-2}(0) + AT^{2\nu}}$$

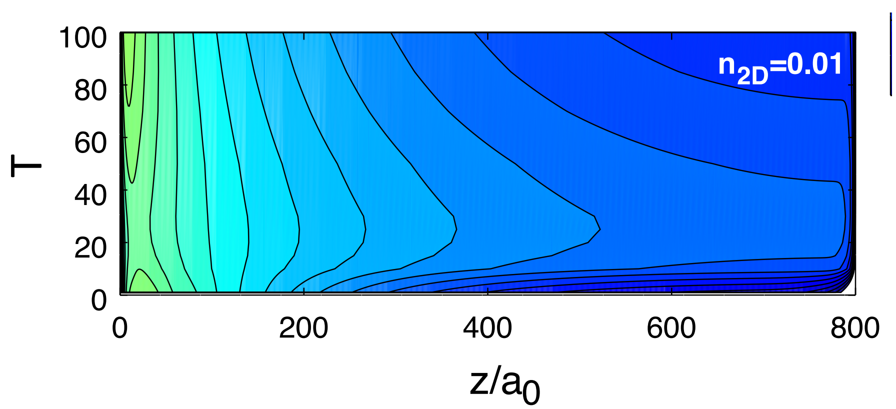

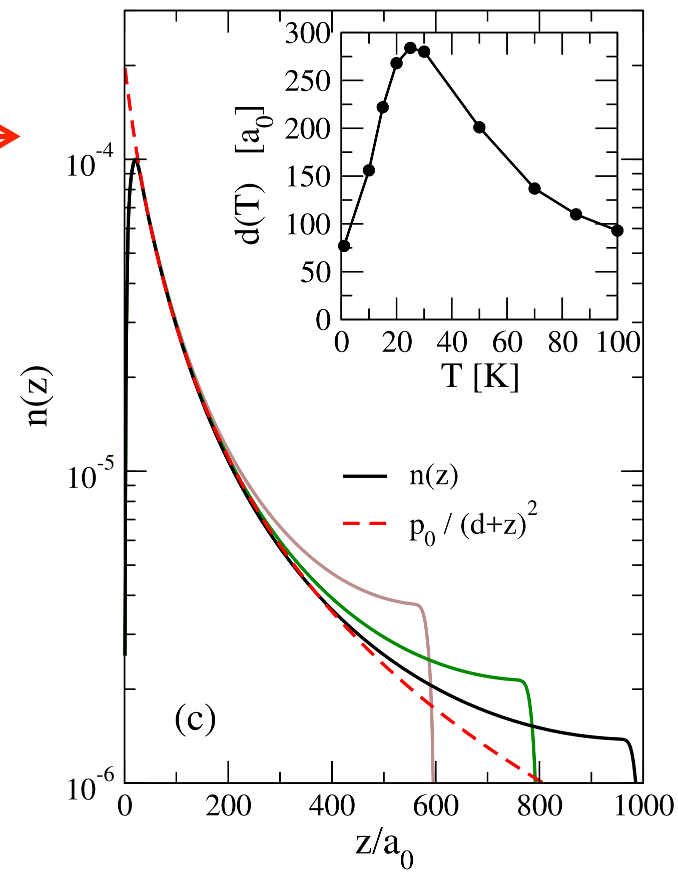

Solution in the weak-field limit:

$$n(z) \approx n_{2D} \frac{\lambda(T)}{\left[\lambda(T)+z\right]^2}$$

$$\lambda(T) = \frac{\varepsilon_\infty 2k_B T \xi(T)^2}{n_{2D} e^2 \xi_0^2} \sim \frac{T}{\xi^{-2}(0) + AT^{2\nu}}$$

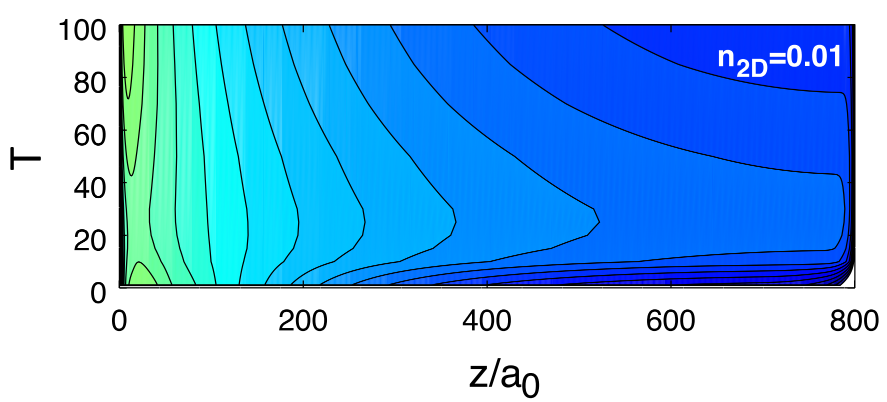

Quantum critical: $\lambda(T) \sim T^{-1}$

Noncritical: *T*-dependence from thermal excitation of QP

FE critical exponents show up in the structure of the tails of the charge distribution.

FIN